Single-spin fluid, spin gap, and d-wave pairing in $YBa_2Cu_4O_8$: A NMR and NQR study

M. Bankay, M. Mali, J. Roos, and D. Brinkmann
Physik-Institut, Universität Zürich, 8057 Zürich, Switzerland
(Received 28 March 1994)

We present results of ^{17}O and $^{63,65}Cu$ nuclear magnetic resonance (NMR) and nuclear quadrupolar resonance (NQR) studies in the normal and superconducting state of the 82-K superconductor $YBa_2Cu_4O_8$. The various components of the Cu and O Knight-shift tensors show strong but similar temperature dependences over the temperature range from 8.5 to 300 K in both the CuO_2 planes and the chains, supporting the picture that there is only one spin component in the planes and the chains, although with different susceptibilities. The oxygen data obey the Korringa relation. This may be interpreted as Fermi-liquid behavior of the electronic system far away from the antiferromagnetic wave vector. The temperature dependence of both the planar Cu and O shift tensors and the planar Cu spin-lattice relaxation rate suggest the opening of a pseudo-spin-gap well above T_c. The very different temperature dependence of $1/T_1$ at the planar O and Cu sites points to the reduced role of the antiferromagnetic correlated spin fluctuations at the O site. The data favor the conclusion that $YBa_2Cu_4O_8$ is a d-wave superconductor. Evidence is provided by three data sets: the chain Knight shifts, the ratio of the planar copper and oxygen relaxation rates, and the individual low-temperature behavior of these rates.

I. INTRODUCTION

Over the last several years, nuclear magnetic resonance (NMR) and nuclear quadrupole resonance (NQR) have played an important role in elucidating electronic properties of high-temperature superconductors (HTSC).[1,2] Among the present issues are two main questions. (i) Does a so-called spin-gap exist in the antiferromagnetic (AFM) spin fluctuation spectrum? (ii) Is the orbital motion of the Cooper pairs described by d waves rather than s waves? In this paper we will report Knight shift and NMR/NQR spin-lattice relaxation data for $YBa_2Cu_4O_8$ which provide evidence for the existence of both a spin gap and d-wave pairing. In addition, we will show that in both the planes and the chains a single-spin fluid exists.

The orthorhombic unit cell of $YBa_2Cu_4O_8$ can be considered as two $YBa_2Cu_3O_7$ unit cells joined chain to chain with the second cell displaced $b/2$ along the b axis. Thus, instead of the single Cu-O chains of $YBa_2Cu_3O_7$, the $YBa_2Cu_4O_8$ structure contains double Cu-O chains which form an edge-sharing, square-planar network. The compound is distinguished by its high thermal stability and precise stoichiometry.

There are two copper sites in the $YBa_2Cu_4O_8$ structure: the chain-forming Cu(1) ions are at the center of an oxygen rhombuslike square while the planar Cu(2) ions are five coordinated by an apically elongated oxygen rhombic pyramid. The O(1) ions form the Cu(1)-O(1) chains along the b axis, the O(2) and O(3) [O(2,3) for short] ions are located in the CuO_2 plane, and the apical O(4) bridges the chains and the planes. The Y ions separate CuO_2 planes along the c axis while the Ba ions form the Ba-O(4) planes.

We present measurements of the ^{65}Cu NMR shifts for Cu(1) and Cu(2) over the temperature range from 8.5 to 300 K with a precision several times larger than previously reported in the literature. In addition, O(1) Knight-shift data are presented. Spin-lattice relaxation data were determined for the planar Cu and O sites.

The paper is organized as follows. The next section contains the necessary theoretical NMR/NQR background. Experimental procedures, including the characterization of the sample, are given in Sec. III. In Sec. IV we present and analyze our data, followed by a discussion in Sec. V and a summary in Sec. VI.

II. NMR/NQR THEORY

The Cu and O nuclear spins in $YBa_2Cu_4O_8$ interact with their electronic environment through electric and magnetic hyperfine couplings. In the presence of an applied magnetic field B_0, the Hamiltonian of a nuclear spin I having a quadrupole moment eQ can be written as

$$\mathcal{H} = \mathcal{H}_{\text{Zeeman}} + \mathcal{H}_{\text{quadrupole}} + \mathcal{H}_{\text{hyperfine}} , \qquad (1)$$

where $\mathcal{H}_{\text{quadrupole}}$ arises from the interaction of eQ with the electric field gradient (EFG) tensor present at the nuclear site.

In our NMR experiments, B_0 is large and hence $\mathcal{H}_{\text{quadrupole}} \ll \mathcal{H}_{\text{Zeeman}}$. As a result, for each isotope and each site, the NMR signal is split into a central line arising from the central transition, $(+\frac{1}{2}, -\frac{1}{2})$, and into satellite lines. The $^{63,65}Cu$ nuclei ($I = 3/2$) produce two satellites arising from the $(\pm\frac{1}{2}, \pm\frac{3}{2})$ transitions, while the ^{17}O signal ($I = 5/2$) contains, in addition, two outer satellites due to the $(\pm\frac{3}{2}, \pm\frac{5}{2})$ transitions. Finally, the $\mathcal{H}_{\text{hyperfine}}$ term causes a magnetic shift of each line.

0163-1829/94/50(9)/6416(10)/$06.00

The Hamiltonian $\mathcal{H}_{\text{hyperfine}}$, expressing the *magnetic* coupling between the nuclear spins and their electronic environment, can be viewed as the interaction of a nuclear spin with a time dependent local magnetic hyperfine field H_L generated by the electron spin and the electron orbital motion. The static part of H_L gives rise to the magnetic NMR line shift expressed by the *magnetic shift tensor* K, whose components (in a reference frame $\alpha = x, y, z$), can be decomposed into a spin, an orbital, and a diamagnetic part:

$$K_{\alpha\alpha}(T) = K_{\alpha\alpha}^{\text{spin}}(T) + K_{\alpha\alpha}^{\text{orb}} + K_{\alpha\alpha}^{\text{dia}} . \tag{2}$$

In HTSC compounds, K^{orb} is predominantly temperature independent, whereas the temperature dependent K^{spin} is expected to vanish in the superconducting state due to singlet spin pairing. K^{dia} is small and can be neglected as we will see later.

Each part of the K tensor can be expressed by the respective hyperfine interaction tensor and the *static* electronic susceptibility (i.e., at zero wave vector and zero frequency) as

$$K_{\alpha\alpha}^{\text{spin}} = \frac{1}{g\mu_B} \sum_j (A_j)_{\alpha\alpha} (\chi_j)_{\alpha\alpha}, \tag{3}$$

$$K_{\alpha\alpha}^{\text{orb}} = \frac{1}{\mu_B} O_{\alpha\alpha} \chi_{\alpha\alpha}^{\text{orb}} . \tag{4}$$

For the analysis of the O(2,3) data, we introduce the following notations. K_c denotes the tensor component perpendicular to the CuO_2 planes ($B_0 \parallel c$), while the in-plane components of the shift are given by $K_\parallel$ and $K_\perp$, where B_0 is parallel and perpendicular to the CuO-bond axis, respectively. K^{spin} at the oxygen sites is due to the spin density on the $2p$ and $2s$ states. The hyperfine field from the $2p$ states is predominantly the anisotropic spin dipolar field, whereas from the $2s$ states it is the isotropic contact field. By defining the axial spin part of K, $K_{\text{ax}}^{\text{spin}}$, as

$$K_{\text{ax}}^{\text{spin}} = \frac{K_\parallel^{\text{spin}} - K_\perp^{\text{spin}}}{3} , \tag{5}$$

we get a shift contribution which couples exclusively to the $2p$ states. The equivalent definition for the isotropic spin part of K is

$$K_{\text{iso}}^{\text{spin}} = \frac{K_\parallel^{\text{spin}} + K_\perp^{\text{spin}} + K_c^{\text{spin}}}{3} . \tag{6}$$

The fluctuating part of H_L is the source of the nuclear spin-lattice relaxation. In HTSC compounds, the main contribution to the copper and oxygen spin-lattice relaxation stems from the electron spin fluctuations. After Moriya,[3] this contribution is related to the imaginary part of the dynamical spin susceptibility $\chi(\vec{q}, \omega_0)$, and the "relaxation rate per temperature unit" $(T_1T)^{-1}$ is given by

$$\left(\frac{1}{T_1T}\right)_\alpha = \frac{\gamma_n^2 k_B}{2\mu_B^2} \sum_{\vec{q}, \alpha' \neq \alpha} |A(\vec{q})_{\alpha'\alpha'}|^2 \frac{\chi''_{\alpha'\alpha'}(\vec{q}, \omega_0)}{\omega_0} , \tag{7}$$

$$A(\vec{q})_{\alpha\alpha} = \sum_j A_{j,\alpha\alpha} \exp(i\vec{q} \cdot \vec{r}_j) .$$

Here, ω_0 is the nuclear resonance frequency, α denotes the direction of quantization, i.e., the direction of V_{zz} in NQR and of B_0 in NMR experiments, and α' is the direction perpendicular to α. A_j is the on-site ($\vec{r}_j = \vec{0}$) and the transferred ($\vec{r}_j \neq \vec{0}$) hyperfine coupling tensor for the nuclei under consideration. Thus, the "relaxation rate per temperature unit" provides information about the $\vec{q}$ averaged imaginary part of $\chi(\vec{q}, \omega_0)$.

III. EXPERIMENTAL

The $YBa_2Cu_4O_8$ sample, investigated in this work, was prepared by the solid state reaction technique, which is described in detail elsewhere.[4]

Only ^{17}O, which possesses a nuclear spin, is suitable for oxygen NMR experiments. Since the ^{17}O abundance is only 0.037%, it is necessary to prepare ^{17}O enriched samples.

The ceramic pellets of $YBa_2Cu_4O_8$ were synthesized from a mixture of prereacted $YBa_2Cu_3O_7$ and CuO under an O_2 pressure of 400 bar. After a reaction time of 20 h at a temperature of 1040 °C, the $YBa_2Cu_4O_8$ material was cooled down to room temperature at a cooling rate of 2 °C/min. The sample was then charged into an Al_2O_3 crucible and consequently placed in a quartz-pyrex reaction chamber, to which the ^{17}O container was sealed. After evacuation of the whole setup to a pressure of 10^{-3} mbar, the break seal was fractured and ^{17}O gas was allowed to enter the reaction chamber, where a pressure of nearly 1 bar was reached. The ^{17}O annealing took place at a temperature of 810 °C for 500 h.

X-ray diffraction measurements found the existence of small amounts of CuO and high-pressure Ba-cuprate as impurity phases. dc magnetization experiments at 14 Oe showed a clear decrease of the susceptibility at 81 K and a Meissner fraction of 36%.

In order to study the anisotropic properties of the $YBa_2Cu_4O_8$ compound, the Cu and O NMR experiments were carried out on a c-axis-oriented powder. The magnetic orienting of the powder, described in Ref. 5, produced a sample with a high degree of c-axis alignment of the grains whereas a and b axes remained randomly distributed.

The $^{63,65}Cu$ NQR and NMR experiments were performed by using standard pulsed spectrometers. The resonance signals were obtained by a phase-alternating add-subtract spin-echo technique similar to that one used in Ref. 6.

The NQR measurements were done in zero magnetic field. The spectra were obtained by scanning the frequency in discrete steps and integrating the echo signal. The NMR experiments were performed in an external magnetic field B_0 of 9.03 T using Fourier transformation of the spin echo.

The spin-lattice relaxation time T_1 was measured by NQR and NMR using the inversion-recovery pulse sequence. In all our experiments we used very intense radiofrequency pulses with optimal pulse lengths of 1.5 μs or less.

IV. RESULTS AND ANALYSIS

A. Cu(1) and Cu(2) linewidths

All determinations of the Cu linewidth and Knight shift were done on the central signals. In order to do so we fitted the asymmetrically broadened spectra by a line shape function that involves the convolution of a Gaussian and a Lorentzian. The nearly temperature independent Gaussian describes the angular distribution of c-axis misalignment, responsible for an asymmetric second order quadrupolar shift broadening of the resonance lines towards lower frequencies.[7] The temperature dependent line broadening present at each orientation is taken into account by the Lorentzian. The Gaussian distribution is adjusted for small temperature effects.

The Cu(1) NMR line at the orientation $B_0 \parallel c$ is very narrow as shown in the inset of Fig. 1. The solid line represents the model line shape. The Gaussian width is about 4° reflecting the good orientation of the powder. For $B_0 \perp c$, the Cu(1) spectrum represents a powder pattern and hence the lines are much broader, in the range of MHz. In analyzing these spectra, we filtered the calculated powder pattern with the excitation spectrum of the radiofrequency pulse.

The Cu(2) NMR line at the orientation $B_0 \perp c$ is much smaller than the corresponding Cu(1) line, namely, 26 kHz, because of the nearly axially symmetric EFG at the Cu(2) site. Its asymmetry parameter η is 0.015.

The Lorentzian linewidth of all these lines increases with decreasing temperature as already reported for the Cu(1) and Cu(2) lines in $YBa_2Cu_3O_7$.[8] As shown in Fig. 1, the temperature dependence of the Cu(1) line at $B_0 \parallel c$ is well described by the Néel-like function $\Gamma(T) = a/(b+T)$ with a= 2.8 K MHz and b= 14.9 K. The reason for this behavior is still unknown; there seems to be an ordering of the spins with decreasing temperature. Be that as it may, $\Gamma(T)$ also fits the linewidths of the Cu(1) and Cu(2) signals for the orientation $B_0 \perp c$.

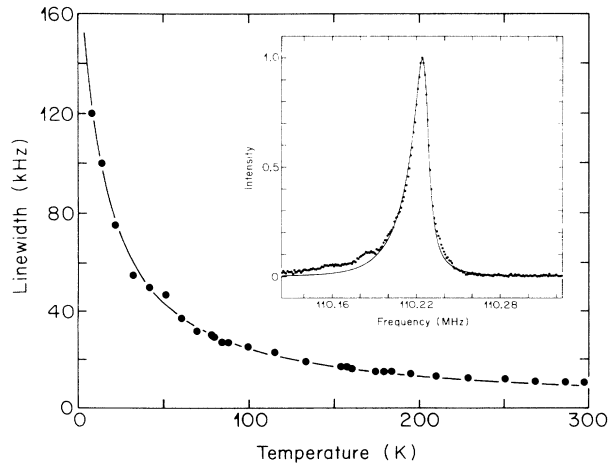

FIG. 1. Inset, the ^{65}Cu(1) central line is shown with the field oriented along the c axis for T = 300 K. The solid line represents a fit to the data (see text). Main figure: linewidths of the ^{65}Cu(1) central line vs temperature (with $B_0 \parallel c$), fitted by a Néel-like temperature behavior discussed in the text.

B. Temperature dependence of Cu and O Knight shifts

Due to demagnetizing currents, the magnetic field inside a type-II superconductor which is in the superconducting state is not equal to the applied magnetic field. Therefore, accurate $K(T)$ data can only be obtained if the magnetic field inside the sample is known. Figure 2 shows that the magnetic shift tensor for the plane Cu(2) site, K_c, is constant within an error of 0.003% in the temperature range 36 K to 300 K. This result implies that, according to Eq. (2), the shift for this orientation is entirely of orbital origin and, in addition, that the diamagnetic shift in the superconducting phase is smaller than 0.003%. Hence we do not have to correct the K data because of a possible difference between internal and external magnetic field.

On the other hand, K_{ab} shows a significant temperature dependence in the normal state similar to $YBa_2Cu_3O_{6.63}$. Both compounds exhibit remarkable quantitative similarities as their K values differ by only 10% in the temperature range we have studied. According to Eq. (5), K_{ab} must have the same temperature dependence as K_{ax}.

The temperature dependence of the shift tensor for the Cu(1) site is given in Fig. 3. In the normal conducting state, all three components of K decrease linearly with temperature over a range of 220 K. Below T_c, K_c and K_b decrease with decreasing temperature while K_a is almost constant because the spin susceptibility is very small for this orientation.

Walstedt *et al.*[9] have reported a qualitatively similar decrease of K_c in the normal state of $YBa_2Cu_3O_7$ provided the shift is extracted from the NMR signal's center position, while an evaluation of the signal's center of gravity yields different values. On the other hand, in contrast to $YBa_2Cu_4O_8$, in the superconducting phase of $YBa_2Cu_3O_7$ all three components of the shift tensor

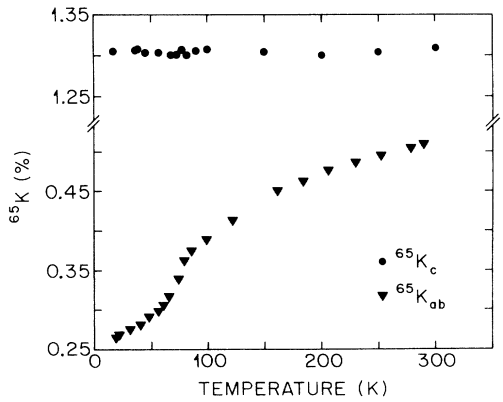

FIG. 2. The total magnetic shift as a function of temperature for ^{65}Cu(2) with $B_0 \parallel c$ (circles) and $B_0 \perp c$ (triangles).

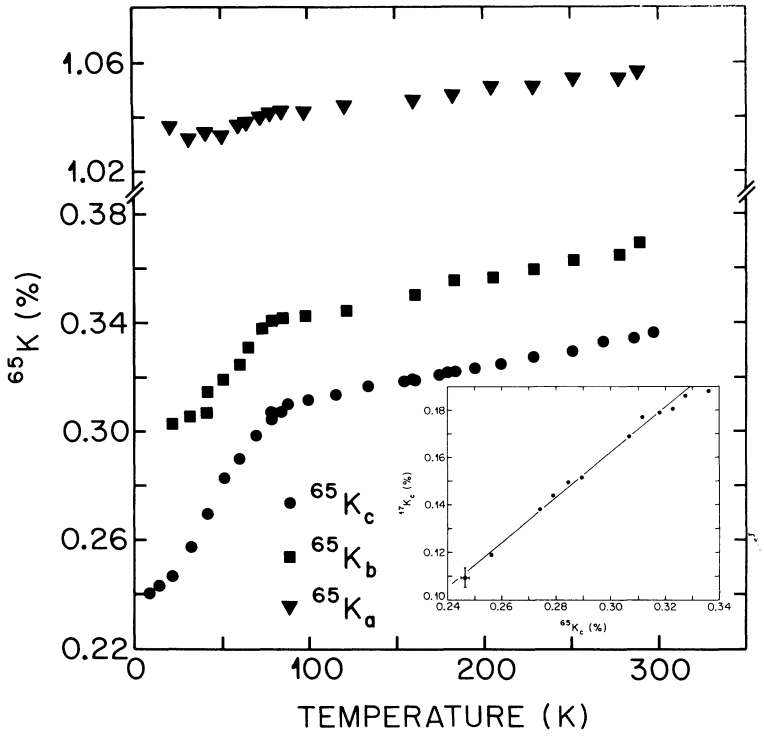

FIG. 3. The total magnetic shift as a function of temperature for ^{65}Cu(1) with $B_0 \parallel a$ (triangles), $B_0 \parallel b$ (squares), and $B_0 \parallel c$ (circles). Inset: ^{17}O(1) shift plotted vs ^{65}Cu(1) shift.

exhibit almost the same decrease.[10,8]

For the oxygen shift data, we have extended our previous measurements[11] into the superconducting state. All components of the chain oxygen O(1) shift (see Fig. 4) exhibit about the same temperature dependence in the normal phase. The assignment of the various ^{17}O signals to the oxygen sites and the identification of the EFG tensor axes (at 100 K) were discussed in Ref. 11; the procedure utilized the results of an EFG calculation.[12] However, for the chain O(1) site the assignment of the EFG components and hence of the shift components K_a and K_b along the a and b directions is ambiguous since the theoretical EFG values are the same, except for a sign, while the experimental values differ by 7%. We have now assigned the K_a and K_b shifts in such a way that the qualitative temperature dependence of all three O(1) shift components agrees with the respective Cu(1) components.

C. Spin-lattice relaxation

We have measured the temperature dependence of the spin-lattice relaxation time for both the planar Cu(2) and the planar O(2,3) sites with the magnetic field $B_0 \parallel c$. The measurements were made on the high-frequency quadrupole satellites to ensure that only signals of the O(2,3) and Cu(2) sites, respectively, were detected.

Figure 5 shows the results for the quantities $^{17}(T_1T)^{-1}$

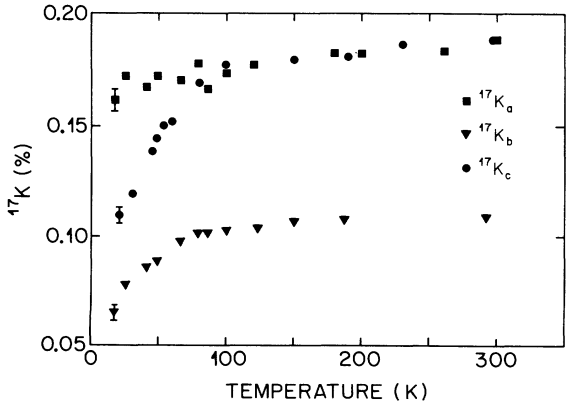

FIG. 4. The total magnetic shift as a function of temperature for ^{17}O(1) with $B_0 \parallel b$ (triangles), $B_0 \parallel a$ (squares), and $B_0 \parallel c$ (circles).

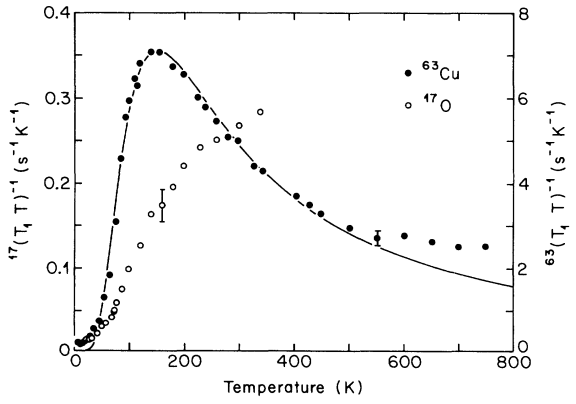

FIG. 5. Temperature dependence of $(T_1T)^{-1}$ at Cu(2) (solid circles) and O(2,3) (open circles) with $B_0 \parallel c$. The solid line is a fit of the data to the spin-gap function Eq. (11); see text.

and $^{63}(T_1T)^{-1}$. Both the Cu and the O data display a strong temperature dependence already above T_c in contrast to the temperature independent behavior found in most metals. With falling temperature, $^{17}(T_1T)^{-1}$ is a monotonic decreasing function, whereas $^{63}(T_1T)^{-1}$ first increases down to about 130 K and then rapidly decreases. It is interesting to note that in the same temperature regime $^{63}(T_1T)^{-1}$ exceeds $^{17}(T_1T)^{-1}$ by as much as a factor of 20. The relaxation mechanisms for both the O(2,3) and Cu(2) nuclei are of magnetic origin.

V. DISCUSSION

In discussing our results we will focus on four aspects: the spin-fluid model, the spin-gap effect, the *d*-wave pairing symmetry, and the Korringa relation.

A. Single-spin fluid model

The new measurements of the planar Cu and O Knight shifts enlarge our previous data[11] and improve our recent measurements.[2] The major result of these studies is the fact that the various shift components exhibit the same temperature dependence over a large temperature range extending from 8.5 K to about 300 K with a decline which starts already well above T_c (Fig. 6). These facts support the "single-spin fluid" model which states that the Cu 3*d* holes and the doped holes (which mainly go into O 2*p* states) have one spin degree of freedom. Our $YBa_2Cu_4O_8$ shift data are very similar to those for $YBa_2Cu_3O_{6.63}$,[13] which demonstrates once again the similarity of both compounds in terms of hole doping: both compounds are underdoped, which means their doping level is below the value corresponding to a maximum T_c. On the other hand, the slight increase, with falling temperature, of the planar O shift in $YBa_2Cu_3O_7$ is recognized as the signature of slightly overdoped samples.[14]

Similar ^{17}O shift data for $YBa_2Cu_4O_8$ have been reported by Machi *et al.*[15] and similar Cu Knight-shift data were obtained in $Bi_2Sr_2CaCu_2O_8$.[16] Strong evidence for the single-spin fluid model has also been provided by ^{89}Y NMR.[17]

Turning now to the chain site Knight shifts, we first note that all components of both the Cu(1) and O(1) shift decrease below T_c although this is less pronounced for the K_a component. The second observation is that all K components of Cu(1) are proportional to the respective component of O(1) as shown in the inset of Fig. 3. This demonstrates that not only the planes but also the chains form a single-spin fluid. However, the susceptibilities of the two systems are different.

B. Spin-gap effect

We will now discuss how the temperature dependence of the Knight shift and the spin-lattice relaxation provide evidence for the existence of a spin gap. We will begin with a discussion of our data in terms of the Millis-Monien-Pines (MMP) phenomenological model[18] which provides a good starting point for describing spin-lattice relaxation in the normal state. One of the essential assumptions of the model is that the electron susceptibility, $\chi(\vec{q},\omega)$, which enters into the Moriya formula Eq. (7), consists of two additive parts, the first one describing the quasiparticle (normal Fermi-liquid-like) contribution and the second one the AF correlations.

Within the MMP model, we can qualitatively explain the markedly different normal-state temperature dependence of $^{63}(T_1T)^{-1}$ at the Cu(2) site and of $^{17}(T_1T)^{-1}$ at the O(2,3) site in terms of the *one*-spin component model with a *single* dynamic susceptibility $\chi(\vec{q},\omega)$ arising from *one* spin degree of freedom as proposed in Refs. 18–21. The various nuclei scan different $\vec{q}$ regions of the same $\chi(\vec{q},\omega)$ at ω_0. The Cu nucleus samples the spin fluctuations of the entire $\vec{q}$ space, and $^{63}(T_1T)^{-1}$ is greatly enhanced by the AF-correlated spin fluctuations, which are peaked at $\vec{Q}_{AF} = (\frac{\pi}{a}, \frac{\pi}{a})$, as found from neutron scattering experiments.[22,23] On the other hand, $^{17}(T_1T)^{-1}$ is

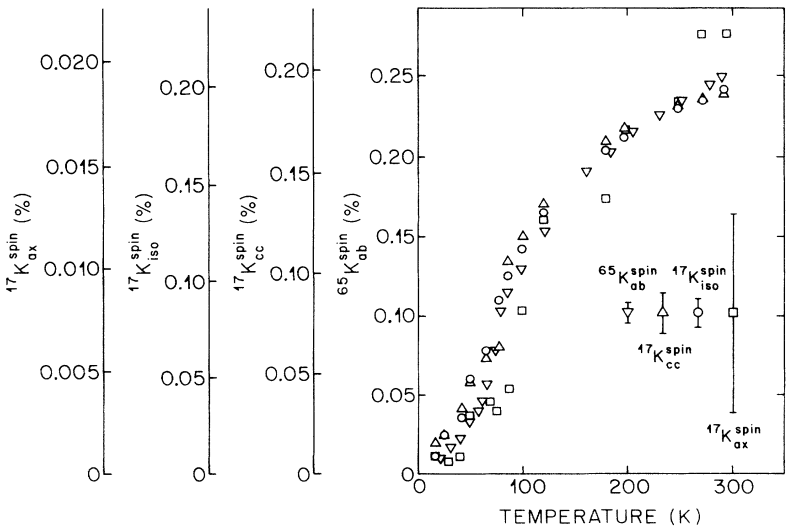

FIG. 6. Various Knight-shift components of O(2,3) and Cu(2) are plotted vs temperature (with different vertical scales).

determined by the fluctuations at $\vec{q} \neq \vec{Q}_{\rm AF}$, owing to the fact that the AF-correlated spin fluctuations are filtered out at the geometrically symmetric O site.

$^{63}(T_1T)^{-1}$ at Cu(2) exhibits a maximum well above T_c, namely, at $T \approx 130$ K (see Fig. 5). This has also been observed in oxygen-deficient $YBa_2Cu_3O_{6+x}$ materials [$x = 0.5$,[14] $x = 0.6$ (Ref. 13)], but not in $YBa_2Cu_3O_7$,[14] where $^{63}(T_1T)^{-1}$ starts to decrease close to T_c. Neutron scattering experiments in $YBa_2Cu_3O_{6.5}$ at $\vec{q} \approx \vec{Q}_{\rm AF}$ indicate[23] that the decrease of $^{63}(T_1T)^{-1}$ above T_c is due to the opening of a spin gap in the magnetic excitations. When spectral weight in the spin fluctuations decreases as the temperature is lowered, then the missing weight must reappear at a higher energy in the form of a transition over a "spin pseudogap." The energy of the spin gap strongly depends on the doping level of the material.[23] The opening of the spin gap *above* T_c, expressed by the maximum in $^{63}(T_1T)^{-1}$ above T_c, is like a fingerprint for underdoped HTSC materials such as $YBa_2Cu_4O_8$, $YBa_2Cu_3O_{6+x}$ ($x < 0.94$), $Y_2Ba_4Cu_7O_{15}$,[24] and $La_{2-x}Sr_xCuO_4$.[25]

The physical origin of the spin gap is still under debate. Within the Hubbard[26] and the t-J model,[27] the spin gap is caused by the nesting property of the Fermi surface whereas according to Ref. 28 it is a direct consequence of the narrow conduction band. In the revised version of the MMP model,[21] the appearance of a spin gap follows from the temperature behavior of the energy of the spin fluctuations around $\vec{Q}_{\rm AF}$.

Tranquada *et al.*[29] found that their neutron scattering data for $YBa_2Cu_3O_{6.6}$ could be described, in the presence of a spin gap, by a phenomenological expression for the susceptibility of the form

$$\chi''(\omega) = A\left[\tanh\left(\frac{\hbar(\omega-\omega_g)}{2k_BT}\right) + \tanh\left(\frac{\hbar(\omega+\omega_g)}{2k_BT}\right)\right], \tag{8}$$

where A is a constant and ω_g is the experimental gap frequency. If one assumes that Eq. (8) is applicable to NMR data where $\hbar\omega \ll k_BT$, one obtains

$$\chi''(\omega \approx 0) = BT^{-1}\left[1 - \tanh^2\left(\frac{\Delta}{2T}\right)\right], \tag{9}$$

where we have introduced the spin gap $\Delta = \hbar\omega_g/k_B$. Some applications of Eq. (9) to Knight shift and relaxation rates are discussed in Ref. 30 and Ref. 2. Here, we will first continue the discussion of the Knight shift which probes the spin fluctuations at zero wave vector.

We have fitted the normal-state Cu(2) Knight-shift data in $YBa_2Cu_4O_8$ by a formula which contains the essential tanh term of Eq. (9):

$$\chi(0,0) = \chi_0\left[1 - \tanh^2\left(\frac{\Delta_0}{2T}\right)\right], \tag{10}$$

which is the temperature dependent factor of the shift [see Eq. (3)]. We obtained $\Delta_0 = (180 \pm 10)$ K which is in good agreement with the neutron scattering result. If the temperature variation of the Knight shift is really due to the opening of a spin gap and Eq. (10) is appropriate for analyzing the data, the results imply that a spin gap Δ_0 opens also at $\vec{q} = \vec{0}$.

The discussion of the Knight shift in the superconducting state is intimately connected with the issue of the pairing-state symmetry and hence will be postponed to the next section.

In discussions of the spin-lattice relaxation rate in terms of the spin-gap effect it became customary[2,30,24] to describe the relaxation rate by the *ad hoc* formula

$$\frac{1}{T_1T} = \left(\frac{A_0}{T}\right)^{\alpha}\left[1 - \tanh^2\left(\frac{\Delta_{\rm AF}}{2T}\right)\right]. \tag{11}$$

Here, A_0 is a constant. $\Delta_{\rm AF}$ denotes the spin-gap energy at the $\vec{Q}_{\rm AF} = (\frac{\pi}{a}, \frac{\pi}{a})$ since the Cu relaxation is dominated by the strong AF fluctuations around $\vec{Q}_{\rm AF}$. Instead of the constant prefactor χ_0 of Eq. (10), the factor $T^{-\alpha}$ is introduced, which guarantees a reasonable description for the high-temperature behavior and may be attributed to the gradual decay of AF correlations at higher temperatures.[18,21]

Figure 5 shows the fit of Eq. (11) to the Cu(2) relaxation rates in $YBa_2Cu_4O_8$ yielding the parameters $\Delta_{\rm AF} = (280 \pm 20)$ K and $\alpha = 1.4$. It is remarkable that the result agrees (within the error limits) with the parameters obtained from fitting Eq. (11) to the relaxation rates of *both* planar sites, Cu(2) and Cu(3), in $Y_2Ba_4Cu_7O_{15}$.[24] This demonstrates the very similar spin dynamics in $YBa_2Cu_4O_8$ and $Y_2Ba_4Cu_7O_{15}$ and that the doping levels of the blocks in $Y_2Ba_4Cu_7O_{15}$ are close to optimal doping.[24]

C. Spatial symmetry of pairing state

We will now address the question whether spin-lattice relaxation and Knight shift provide evidence for a certain spatial symmetry of the pairing state. There are several ways to check this symmetry with the aid of NMR/NQR data.

1. Evaluation of Knight-shift data

It is usually assumed[31] that the susceptibility of the superconducting state, χ_s, is related to the normal-state susceptibility, χ_n, which is taken as temperature *independent*, via

$$\chi_s(T) = Y_l(T)\chi_n, \tag{12}$$

where

$$Y_l(T) = \int_{-\infty}^{\infty} N_l(E)\left(-\frac{\partial f}{\partial E}\right)dE \tag{13}$$

is a function which depends on the angular momentum l involved in the pairing. $N(E)$ is the superconducting density of states and f is the Fermi distribution function. It is $Y_l(T)$ which determines the variation of the Knight shift with temperature. For $l = 0$, $Y_0(T)$ is called the Yosida function;[32] it describes the conventional BCS weak-coupling spin-singlet s-wave pairing mechanism.

In fitting our Cu(2) shift data for the superconducting state (see Fig. 7), we made the additional assumption that the spin-gap function Eq. (10) is also applicable to the superconducting state if χ_0 is replaced by $Y_l(T)\chi_0$. Unfortunately, the calculations of $Y_l(T)$ for $l \neq 0$ are more involved and no results are available for $YBa_2Cu_4O_8$. Thus, using $Y_0(T)$ we restricted our fit to s-wave pairing only.

For comparison, the inset of Fig. 7 shows the corresponding Cu(2) data for $YBa_2Cu_3O_7$ (Ref. 33) fitted by Eq. (13) for $l = 0$ (s wave) and $l = 2$ (d wave). Note, that for $YBa_2Cu_3O_7$ there is no need to apply the spin-gap function because the normal-state shift in the overdoped $YBa_2Cu_3O_7$ compound is nearly constant or even slightly increasing with falling temperature. The precision of the experimental data is not sufficient to allow an unambiguous decision whether s- or d-wave pairing is present. The same statement applies to our $YBa_2Cu_4O_8$ data as long as a calculation of $Y_2(T)$ is missing.

For the K_c shift data of the chain Cu(1) site the situation is more promising. Figure 8 shows a fit of the Yosida function to our data in $YBa_2Cu_4O_8$; the corresponding data for $YBa_2Cu_3O_7$ (Ref. 34) are given in the inset. For both compounds, the s-wave fit is not satisfactory and the $YBa_2Cu_3O_7$ data can be fitted perfectly with the d-wave expression. It remains to be seen whether the same conclusion applies to $YBa_2Cu_4O_8$.

Finally, we wish to stress the issue whether the decrease of the chain Knight shifts in both compounds is merely due to a proximity effect[34] or whether it reflects some participation of the chains in superconductivity.

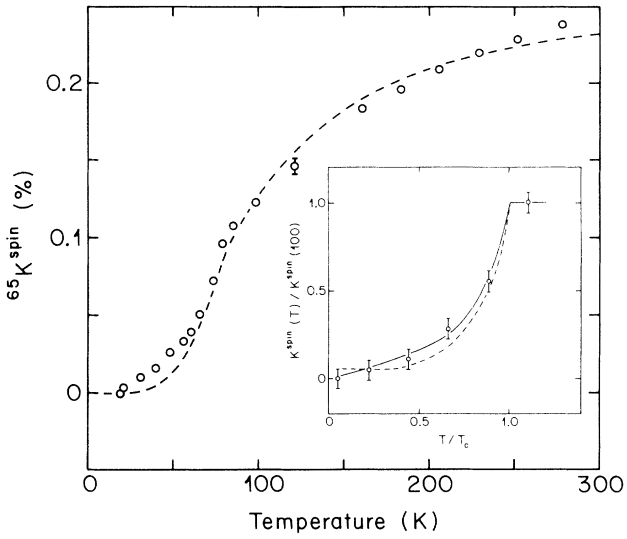

FIG. 7. Temperature dependence of the Cu(2) Knight shift in $YBa_2Cu_4O_8$ with $B_0 \perp c$. The dashed line is the spin-gap function Eq. (10) multiplied (below T_c) by the Yosida function as calculated for BCS, weak-coupling, spin-singlet, $L = 0$ pairing. Inset: normalized Cu(2) Knight shift in $YBa_2Cu_3O_7$ with $B_0 \perp c$. Theoretical curves are from the Monien and Pines evaluation of Eq. (13) for BCS spin-singlet s-wave (dashed line) and d-wave (solid line) pairing (from Ref. 33).

2. *Evaluation of relaxation data*

Spin-lattice relaxation data offer several ways to check the symmetry of the pairing state. One possibility is to measure the anisotropy $r = {}^{63}T_1^c/{}^{63}T_1^{ab}$ of the Cu relaxation rate in the superconducting state where c and ab specify the orientation of the applied magnetic field B_0. Detailed theoretical analyses[35–38] of the relaxation data for $YBa_2Cu_3O_7$ (Refs. 39 and 40) revealed that the temperature variation of r is not compatible with s-wave pairing and favors d-wave symmetry.[2] Our $YBa_2Cu_4O_8$ data[41] are in qualitative agreement with the $YBa_2Cu_3O_7$ data and thus also favor d-wave symmetry.

However, these theoretical approaches were not capable of explaining the ^{17}O relaxation rate[42] and, hence, the relaxation rate ratio $^{17}T_1^c/{}^{63}T_1^c$, which is a mea-

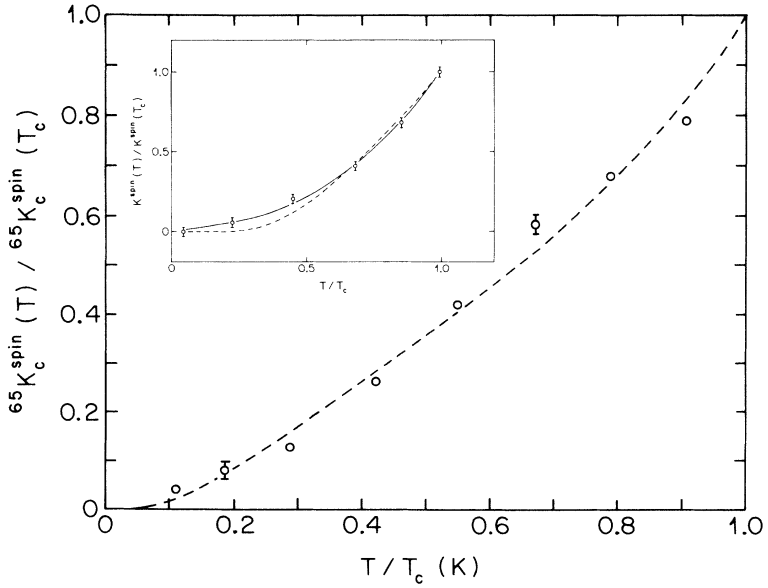

FIG. 8. Temperature dependence of the normalized Cu(1) Knight shift in $YBa_2Cu_4O_8$ (main figure) and $YBa_2Cu_3O_7$ (inset; from Ref. 34) for $B_0 \parallel c$. Dashed line: fit by Yosida function as calculated for BCS, weak-coupling, spin-singlet, $L = 0$ pairing. Solid line: fit by spin-singlet, orbital d-wave, pairing state.

sure for the enhancement of the Cu relaxation rate by AF-correlated spin fluctuations as mentioned above. The theory predicted either a nearly temperature independent value or an increase of the ratio at lower temperature.[36] However, these calculations had assumed a closed Fermi surface for $YBa_2Cu_3O_7$ while photoemission experiments had revealed an open Fermi surface. Thelen *et al.*[42] extended their calculations by including next-nearest-neighbor hopping of the quasiparticles and assuming an open Fermi surface. In this way they succeeded in fitting the $YBa_2Cu_3O_7$ data of Martindale *et al.*[43] with a $d_{x^2-y^2}$-wave rather than an s-wave pairing state.

Figure 9 plots the temperature dependence of the $^{17}T_1^c/^{63}T_1^c$ ratio for $YBa_2Cu_4O_8$ in the normal and superconducting state with $B_0 \parallel c$. $^{63}T_1^c$ was measured by NQR and $^{17}T_1^c$ by NMR at 9.03 T. The ratio increases with falling temperature in the normal state, reaches a maximum of 65 at T_c, and then decreases linearly down to 22 K. This result is in good agreement with data by Tomeno *et al.*,[44] who measured down to 40 K and obtained a maximum value of 53. However, our result disagrees with measurements by Zheng *et al.*[45] which display an *upturn* of the ratio below T_c.

When comparing our result with the $^{17}T_1^c/^{63}T_1^c$ ratio measured in $YBa_2Cu_3O_{6.63}$,[13] which is also underdoped, we note agreement for the normal phase and a slightly lower maximum value of 55 at T_c (which is 62 K). However, the ratio is constant between 47 K (the lowest data point) and T_c.

Finally, comparison with the overdoped $YBa_2Cu_3O_7$ structure shows that here the maximum value of $^{17}T_1^c/^{63}T_1^c$ is only about 23 (Ref. 43) which indicates weaker AF correlations because $YBa_2Cu_3O_7$ is "further away" from the AF phase. Otherwise, the rate ratios in the superconducting phase of both compounds exhibit the essential decrease with falling temperature. However, it should be kept in mind that our oxygen measurements were performed in a high field of 9 T and therefore are not free of magnetic-field effects. Martindale *et al.*[43] have detected a small field dependence of the oxygen rate in $YBa_2Cu_3O_7$, although it does not influence very much the qualitative behaviour of the temperature dependence of the ratio below T_c.

A final clue to the symmetry of the pairing state is provided by the individual behavior of the relaxation rates in the superconducting state. We note that both the planar Cu and O rates show no coherence peak just below T_c, nor does the rate diminish exponentially with decreasing temperature as observed in conventional s-wave superconductors. Instead, the temperature dependence of $1/T_1$ is rather power-law-like, i.e., $1/T_1 \propto T^n$ with n between 2.5 and 3 (see Fig. 10). This points to the existence of nodes in the superconducting gap as one expects, for instance, for d-wave pairing superconductivity.[36]

D. The Korringa relation for planar oxygen

A much debated question in NMR/NQR studies of HTSC's is whether the planar oxygen relaxation time and the Knight shift satisfy the Korringa relation, which states that $T_1TK_{\rm spin}^2 = \kappa(\hbar/4\pi k_B)(\gamma_e/\gamma_n)^2$ where $\kappa = 1$ for the free-electron model.

We have reanalyzed our previous oxygen magnetic shift data[11] and have plotted in Fig. 11 both $(TT_1)^{-1/2}$ and (TT_1) as a function of $K_{\rm spin}$. In this way it is possible, without knowing the orbital shift, to find out whether the Korringa relation is obeyed or whether instead the product $T_1TK_{\rm spin}$ is constant. Although both plots reveal a linear relationship, it is only the $(T_1T)^{-1/2}$ plot that yields, when extrapolated to $(T_1T)^{-1/2} = 0$, orbital shifts that agree, within experimental errors, with the extrapolation of the measured shifts to zero temperature. These orbital shifts are $K_{cc}^{\rm orb} = (-0.031 \pm 0.008)\%$, $K_{\parallel}^{\rm orb} = (-0.009 \pm 0.008)\%$, and $K_{\perp}^{\rm orb} = (-0.023 \pm 0.008)\%$. Using the Korringa relation, we then obtained $\kappa = 1.34$ which is in good agreement with $\kappa = 1.4$ for $YBa_2Cu_3O_7$.[46]

Our result is in contrast with studies of both $YBa_2Cu_3O_{6+x}$ (Ref. 13) and $YBa_2Cu_4O_8$,[45,44] which

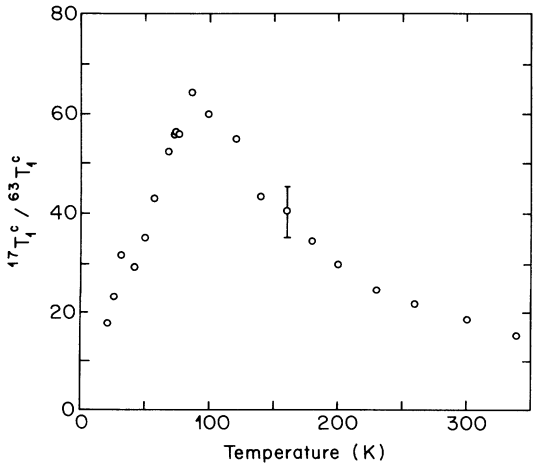

FIG. 9. Temperature dependence of the ratio $^{17}T_1^c/^{63}T_1^c$.

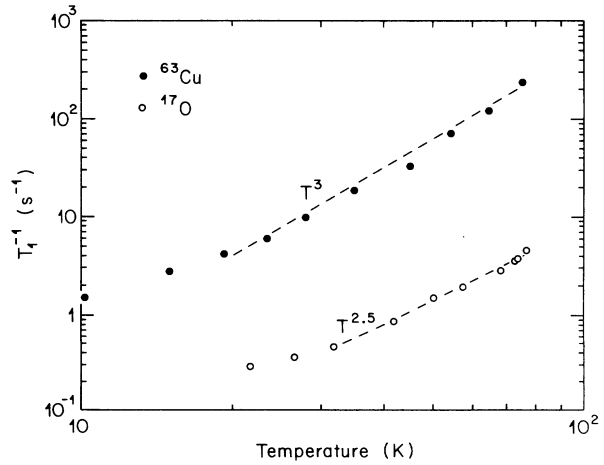

FIG. 10. $(T_1)^{-1}$ vs temperature on a log-log scale for ^{63}Cu(2) (solid circles) and ^{17}O(2,3) (open circles). The dashed lines are fits of power laws to the data.

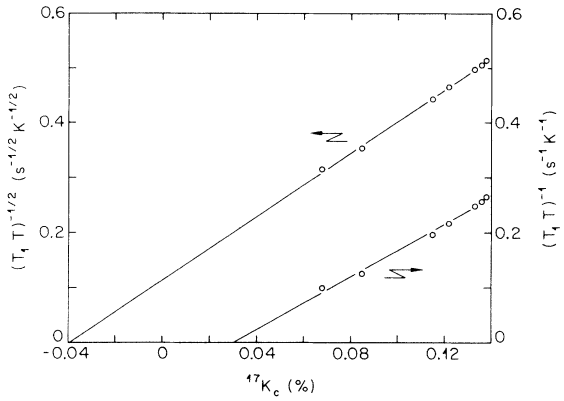

FIG. 11. $(TT_1)^{-1/2}$ and (TT_1) as a function of $K_{\rm spin}$ for O(2,3) with $B_0 \parallel c$.

claim that T_1TK is constant. Horvatić *et al.*[47] found deviations from the T_1TK=const behavior in $YBa_2Cu_3O_{6.52}$ for the field orientation $B_0 \parallel b$ but not for $B_0 \parallel a$.

The reason for these differences is unclear at the moment. Nevertheless, we wish to stress that the decision whether $1/T_1$ is proportional to K or K^2 depends sensitively on the choice of $K_{\rm orb}$. Since the oxygen nuclei sense the electronic system near $\vec{q} = \vec{0}$, the Korringa behavior supports the idea that the electronic systems behave like a Fermi liquid far away from the AF wave vector.

VI. SUMMARY

We have presented Cu and O Knight-shift and spin-lattice relaxation data for $YBa_2Cu_4O_8$. They provide further evidence for the existence of a single-spin fluid in both the CuO_2 planes and the chains, although with different susceptibilities.

The Cu relaxation and Knight-shift data for the CuO_2 planes can be interpreted in terms of a spin gap that opens well above T_c with different gap values for wave vector zero and $(\pi/a, \pi/a)$.

The new data favor the conclusion that $YBa_2Cu_4O_8$ is a d-wave superconductor. Evidence is provided by three data sets: the chain Knight-shift data, the ratio of the planar copper and oxygen relaxation rates, and the individual low-temperature behavior of these rates.

The data for planar oxygen obey the Korringa relation. This may be interpreted as Fermi-liquid behavior of the electronic system far away from the antiferromagnetic wave vector.

ACKNOWLEDGMENTS

We thank the Schweizerischer Nationalfonds for partial support of this work.

[1] C. H. Pennington and C. P. Slichter, in *Physical Properties of High Temperature Superconductors*, edited by D. M. Ginsberg (World Scientific, Singapore, 1990), Vol. 2.
[2] D. Brinkmann and M. Mali, in *NMR Basic Principles and Progress*, edited by P. Diehl (Springer, Berlin, 1994), Vol. 31, p. 171.
[3] T. Moriya, J. Phys. Soc. Jpn. **18**, 516 (1963).
[4] J. Karpinski, E. Kaldis, E. Jilek, S. Rusiecki, and B. Bucher, Nature **336**, 660 (1988).
[5] M. Mali, I. Mangelschots, H. Zimmermann, and D. Brinkmann, Physica C **175**, 581 (1991).
[6] H. Zimmermann, Ph.D. thesis, University of Zurich, Switzerland, 1991.
[7] M. H. Cohen and F. Reif, in *Solid State Physics: Advances in Research and Applications,* edited by F. Seitz and D. Turnbull (Academic, New York, 1957), Vol. 5, p. 321.
[8] S. E. Barrett, D. J. Durand, C. H. Pennington, C. P. Slichter, T. A. Friedmann, J. P. Rice, and D. M. Ginsberg, Phys. Rev. B **41**, 6283 (1990).
[9] R. E. Walstedt, R. F. Bell, L. F. Schneemeyer, J. V. Waszczak, and G. P. Espinosa, Phys. Rev. B **45**, 8074 (1992).
[10] M. Takigawa, P. C. Hammel, R. F. Heffner, Z. Fisk, K. C. Ott, and J. D. Thompson, Phys. Rev. Lett. **63**, 1865 (1989).
[11] I. Mangelschots, M. Mali, J. Roos, D. Brinkmann, S. Rusiecki, J. Karpinski, and E. Kaldis, Physica C **194**, 277 (1992).
[12] C. Ambrosch-Draxl, P. Blaha, and K. Schwarz, Phys. Rev. B **44**, 5141 (1991).
[13] M. Takigawa, A. P. Reyes, P. C. Hammel, J. D. Thompson, R. F. Heffner, Z. Fisk, and K. C. Ott, Phys. Rev. B **43**, 247 (1991).
[14] C. Berthier, Y. Berthier, P. Butaud, W. G. Clark, J. A. Gillet, M. Horvatić, P. Ségransan, and J. Y. Henry, in *Applied Magnetic Resonance*, edited by K. M. Salikov (Springer, Vienna, 1992), Vol. 3, p. 449.
[15] T. Machi, I. Tomeno, T. Miyatake, N. Koshizuka, S. Tanaka, T. Imai, and H. Yasuoka, Physica C **173**, 32 (1990).
[16] R. E. Walstedt, R. F. Bell, and D. B. Mitzi, Phys. Rev. B **44**, 7760 (1991).
[17] H. Alloul, T. Ohno, and P. Mendels, Phys. Rev. Lett. **63**, 1700 (1989).
[18] A. J. Millis, H. Monien, and D. Pines, Phys. Rev. B **42**, 167 (1990).
[19] B. S. Shastry, Phys. Rev. Lett. **63**, 1288 (1989).
[20] F. Mila and T. M. Rice, Physica C **157**, 561 (1989).
[21] A. J. Millis and H. Monien, Phys. Rev. B **45**, 3059 (1992).
[22] J. M. Tranquada and G. Shirane, in *Dynamics of Magnetic Fluctuations in High-Temperature Superconductors*, edited by G. Reiter, P. Horsch, and G. C. Psaltakis (Plenum Press, New York, 1991).
[23] J. Rossat-Mignod, L. P. Regnault, C. Vettier, P. Bourges, P. Burlet, J. Bossy, J. Y. Henry, and G. Lapertot (unpublished).
[24] R. Stern, M. Mali, J. Roos, D. Brinkmann, J. Muller, and Th. Graf (unpublished).
[25] Y. Kitaoka, K. Ishida, S. Ohsugi, K. Fujiwara, and K. Asayama, Physica C **98**, 185 (1991).
[26] N. Bulut and D. J. Scalapino, Phys. Rev. B **45**, 5577 (1992).

[27] D. R. Grempel and M. Lavagna, Solid State Commun. **83**, 595 (1992).
[28] V. V. Moshchalkov and J. Rossat-Mignod (unpublished).
[29] J. M. Tranquada, P. M. Gehring, G. Shirane, S. Shamoto, and M. Sato, Phys. Rev. B **46**, 5561 (1992).
[30] M. Mehring, in *Applied Magnetic Resonance* (Ref. 14), Vol. 3, p. 383.
[31] A. J. Leggett, Rev. Mod. Phys. **47**, 331 (1975).
[32] K. Yosida, Phys. Rev. **110**, 769 (1958).
[33] D. J. Durand, S. E. Barrett, C. H. Pennington, C. P. Slichter, E. D. Bukowski, T. A. Friedmann, J. P. Rice, and D. M. Ginsberg, in *Strong Correlation and Superconductivity*, edited by H. Fukuyama, S. Maekawa, and A. P. Malozemoff (Springer, Berlin, 1989), Vol. 89, p. 244.
[34] C. P. Slichter, S. E. Barrett, J. A. Martindale, D. J. Durand, C. H. Pennington, C. A. Klug, K. E. O'Hara, S. M. DeSoto, T. Imai, J. P. Rice, T. A. Friedmann, and D. M. Ginsberg, in *Applied Magnetic Resonance* (Ref. 14), Vol. 3, p. 423.
[35] N. Bulut and D. J. Scalapino, Phys. Rev. B **45**, 2371 (1992).
[36] N. Bulut and D. J. Scalapino, Phys. Rev. Lett. **68**, 706 (1992).
[37] J. P. Lu, Mod. Phys. Lett. B **6**, 547 (1992).
[38] J. P. Lu and D. Pines (private communication to C. P. Slichter).
[39] J. A. Martindale, S. E. Barrett, C. A. Klug, K. E. O'Hara, S. M. DeSoto, C. P. Slichter, T. A. Friedmann, and D. M. Ginsberg, Phys. Rev. Lett. **68**, 702 (1992).
[40] M. Takigawa, J. L. Smith, and W. L. Hulst, Phys. Rev. B **44**, 7764 (1991).
[41] M. Bankay, M. Mali, J. Roos, I. Mangelschots, and D. Brinkmann, Phys. Rev. B **46**, 11 228 (1992).
[42] D. Thelen, D. Pines, and J. P. Lu, Phys. Rev. B **47**, 9151 (1993).
[43] J. A. Martindale, S. E. Barrett, K. E. O'Hara, C. P. Slichter, W. C. Lee, and D. M. Ginsberg, Phys. Rev. B **47**, 9155 (1993).
[44] I. Tomeno, T. Machi, K. Tai, N. Koshizuka, S. Kambe, A. Hayashi, Y. Ueda, and H. Yasuoka, in *Advances in Superconductivity, Proceedings of the 5th International Symposium on Superconductivity*, edited by Y. Bando and H. Yamauchi (Springer, Kobe, 1992), p. 129.
[45] G.-Q. Zheng, Y. Kitaoka, K. Asayama, Y. Kodama, and Y. Yamada, Physica C **193**, 154 (1992).
[46] P. C. Hammel, M. Takigawa, R. H. Hefner, Z. Fisk, and K. C. Ott, Phys. Rev. Lett. **63**, 1992 (1989).
[47] M. Horvatić, C. Berthier, Y. Berthier, P. Ségransan, P. Butaud, W. G. Clark, J. A. Gillet, and J. Y. Henry, Phys. Rev. B. **48**, 13 848 (1993).